increase our understanding of their importance in osteoarthritis (OA). This study compares the distribution of BMLs with the distribution of denuded bone in a group of OA subjects

**Methods:** 88 individuals were selected from the OAI progression groups 0.B.1 and 1.B.1. The subjects chosen had K-L scores of 2 or 3; medial JSN > lateral JSN, medial osteophytes and ≥1° of varus mal-alignment. OA related bone marrow lesions were defined as poorly delineated region of hyperintensity located in the subchondral bone, excluding the region adjacent to ligament attachment sites. TSE and DESS-we images were manually segmented using EndPoint software (Imorphics, Manchester, UK), with the segmenter blinded as to time point, but not to subject.

A method for measurement of cartilage thickness was adapted to measure the amount of BML adjacent to the bone surface. A statistical model of bone was fitted to each image, generating a set of anatomically corresponded points on the femur, tibia and patella. The amount of BML adjacent to each corresponded point is measured by taking a normal from each point 15mm into the bone and recording the number of BML voxels traversed by the normal. At each point on the surface this provides a measure of BML 'thickness' adjacent to that point. Cartilage thickness was calculated in the same way, using normals projecting out from the bone.

The association of BML and denudation was also measured semi-quantitatively using visualizations as shown in Figure 2. BMLs were scored as either overlapping or adjacent to denuded bone, or not.

The distribution of bone marrow lesions in this population shows a clear pattern (Figure 1). In the femur, BMLs are found predominantly in the patellofemoral joint both medially and laterally, and in the medial femoro-tibial joint. They are almost completely absent in the lateral femoro-tibial joint. In the tibia BMLs are primarily found in the medial tibial compartment. In the patella BMLs are found across the whole joint, with slightly greater density on the lateral facet.

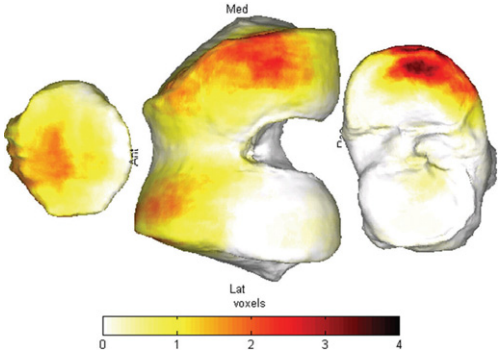


Figure 1. Distribution of BMLs in population. Figure shows average amount of bone marrow lesion across the surface of femur, tibia and patella. Scale is the mean number of BML voxels within 15 mm of the surface.

Table 1. Proportion of BMLs by compartment which overlap or are adjacent to areas of denuded cartilage

| | All | Femur FP | | Femur FT | | Tibia | | Patella | |
|---|---|---|---|---|---|---|---|---|---|
| | | Med | Lat | Med | Lat | MT | LT | MP | LP |
| BMLs which overlap or are adjacent to denuded bobe | 153 | 25 | 19 | 24 | 4 | 50 | 3 | 6 | 22 |
| Total number of BML | 199 | 28 | 27 | 37 | 7 | 53 | 7 | 10 | 30 |
| (%) | (77) | (89) | (70) | (65) | (57) | (94) | (43) | (60) | (73) |

In the baseline images 76.9% of all BMLs either overlapped or were adjacent to denuded bone (Table 1). Figure 2 shows the closeness of this relationship in 6 individuals whose pattern of denudation and BMLs was quite typical for this population. BMLs in the femoro-tibial joint and the lateral tibia overlapped less with denuded but were typically much smaller than those of the patellofemoral joint and patella. Separately we observed that there was no obvious correlation with BMLs and change in cartilage thickness (results not shown); in particular significant cartilage change was not seen in the patellofemoral joint of the femur, or in the patella.

**Conclusions:** A novel method of measurement and display of BMLs demonstrates that there is a striking similarity between the spatial distribution of BMLs and denuded bone in subjects with OA. Application of this method to compare BML with other outcomes may provide greater understanding of structural change in this disease

## 433

### IMPROVEMENT OF THE REPRODUCIBILITY OF THE RADIOGRAPHIC KELLGREN-LAWRENCE (KL) SCORING SYSTEM IN HAND OSTEOARTHRITIS (HOA) USING A NEW KL SCORING SYSTEM AID

**E. Maheu**[1], P. Ravaud[2], G. Baron[2], F. Berenbaum[1], X. Chevalier[3], L. Gossec[4], D. Loeuille[5], J.-F. Maillefert[6], B. Mazières[7], F. Rannou[8], P. Richette[9], C. Cadet[10]

*[1]St Antoine Hosp.-Rheumatology dept- AP-HP, Paris, France; [2]Biostatistics, Bichat Hosp-AP-HP, Paris, France; [3]Rheumatology, Henri Mondor hosp-AP-HP, Creteil, France; [4]Rheumatology B, Cochin Hosp- AP-HP, Paris, France; [5]Rheumatology, Vandoeuvre hosp., Vandoeuvre les Nancy, France; [6]Rheumatology, CHU Dijon, Dijon, France; [7]Rheumatology, CHU Larrey, Toulouse, France; [8]Reeducation dept, Cochin Hosp- AP-HP, Paris, France; [9]Rheumatology, Lariboisière hosp-AP-HP, Paris, France; [10]Rheumatology, Cabinet de rhumatologie, Paris, France*

**Purpose:** KL is the most widely used radiographic scale to define HOA, assess HOA severity and follow-up radiographic progression. Though widely used for case-definition, its interobserver reliability is usually low in HOA.

**Objectives:** To study the impact of a new KL Scoring System Aid (KLSSA) on the reliability of KL scoring.

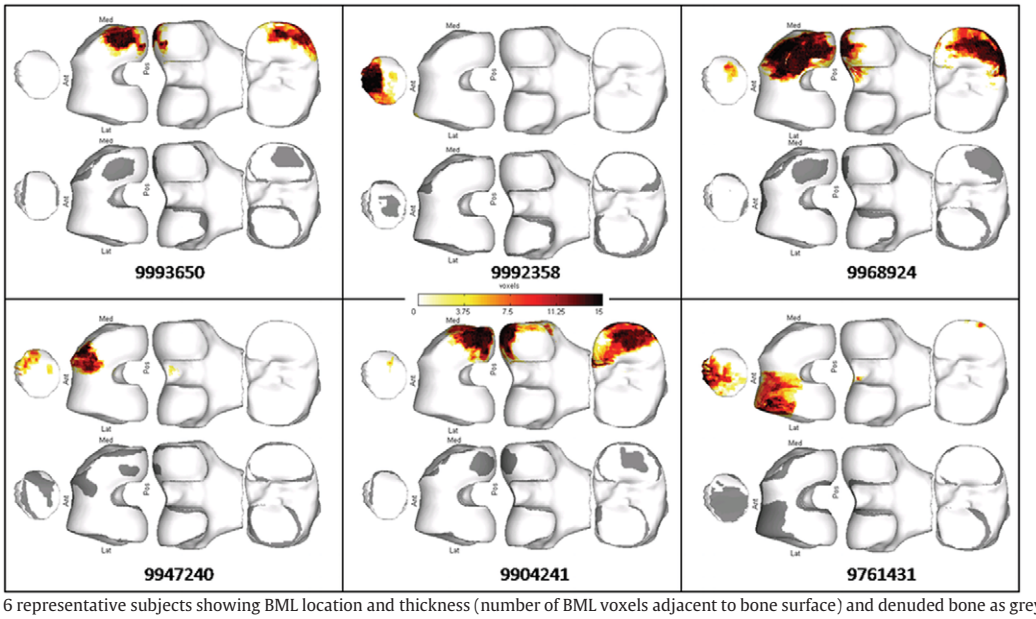


**Abstract 432** – Figure 2. 6 representative subjects showing BML location and thickness (number of BML voxels adjacent to bone surface) and denuded bone as grey mask on the baseline image for each subject.

**Methods:** 20 postero-anterior radiographs of both hands of HOA patients (covering HOA radiographic spectrum) obtained at random from a trial were scored twice by 10 experienced readers at a 15-days interval. Readers were instructed to score the KL (grades: 0-4), using the score as detailed by Kallman [1], and their own view of KL grades. No preliminary training session. During 1st session they also scored joint space narrowing (JSN) and osteophytes (O) (0-4). (Distal (DIP), proximal interphalangeal (PIP), metacarpophalangeal (MCP), scapho-trapezial and trapeziometacarpal joints (16 joints) of one hand selected at random were scored. 8 of the 10 readers (the 2 designers of the KLSSA excluded) were then randomized in 2 groups using the KLSSA or not to score again twice the radiographs, the 4 readers without the KLSSA serving as control group (training effect assessment). The KLSSA combines various amounts of JSN (0-4) and O (0-4) to define KL grades. It shows as a Table, accompanied by HOA images to illustrate the grading. Radiographs were numbered 1-20 at random for each session.
*Statistics:* Intra-class correlation coefficient with 95% confidence interval (CI) for inter- and intraobserver precision; Bland-Altman graphical method for intraobserver precision.
**Results:** Results for interobserver reproducibility appear in the table.

| | 4 readers randomized to score without the KLSSA ICC [CI 95%] | 4 readers randomized to score with the KLSSA ICC [CI 95%] |
|---|---|---|
| Interobserver reproducibility (1st reading) 1st turn before KLSSA use | | |
| Total osteophytes score (0-64) | 0.66 [0.41-0.84] | 0.50 [0.25-0.68] |
| Total JSN score (0-64) | 0.47 [0.27-0.68] | 0.58 [0.34-0.78] |
| Toal KL score (0-64) | 0.51 [0.26-0.72] | 0.41 [0.20-0.64] |
| Interobserver reproducibility (3rd reading) 2nd turn using or not KLSSA | | |
| Total KL score (0-64) | 0.48 [0.25-0.68] | 0.79 [0.59-0.89] |

KLSSA: KL scoring system aid.

Interobserver precision improved in the group using the KLSSA. No training effect was observed. Intra-observer reproducibility improved for the readers not using the KLSSA (0.87 to 0.95) and almost all those using it (0.57 to 0.89). One reader's precision decreased.
**Conclusions:** Interobserver reproducibility of KL radiological grading in HOA was improved by the proposed KLSSA which could help for case definition or radiographic progression assessment in future trials or epidemiological studies. Further work is needed to assess longitudinal reproducibility of KL scoring with this system.
**Acknowledgements:** This work was made possible, thanks to an unrestricted educational grant from Servier Lab.

**Reference**

[1] Kallman. AR 1989;32:1585-91.

## 434

### RAPID MULTI-PLANAR ASSESSMENT OF ARTICLAR CARTILAGE USING HIGH ISOTROPIC RESOLUTION MAGNETIC RESONANCE IMAGING

**R. Kijowski**, J. Klaers, H. Rosas, K. Lee, W. Block
*Univ. of Wisconsin, Madison, WI*

**Purpose:** Balanced steady-state free-precession (SSFP) sequences can be used to evaluate articular cartilage and other joint structures that can be sources of pain in patients with osteoarthritis. At our institution, we have developed a SSFP sequence with high isotropic resolution using alternating repetition time (ATR) fat-water separation and a radial k space trajectory called vastly undersampled isotropic projection reconstruction (VIPR). This study was performed to compare VIPR-ATR with other three-dimensional magnetic resonance imaging (MRI) sequences for evaluating the articular cartilage of the knee joint.
**Methods:** An MRI examination of the knee joint was performed on 7 asymptomatic volunteers and 3 patients with osteoarthritis using a 3 Tesla scanner (GE Healthcare, Waukesha, WI) and an 8-channel phased-array extremity coil. All MRI examinations consisted of the following sequences performed in the sagittal plane: intermediate-weighted FSE-Cube (0.6 mm x 0.6 mm x 0.6 mm voxel size and 5 minute scan time), IDEAL-GRASS (0.4 mm x 0.7 mm x 1.0 mm voxel size and 5 minute scan time), IDEAL-SPGR (0.4 mm x 0.7 mm x 1.0 mm voxel size and 5 minute scan time), VIPR-ATR (0.4 mm x 0.4 mm x 1.2 mm effective voxel size with 3 slice averaging of 0.4 mm isotropic images in each dimension and 5 minute scan time), and high resolution (HR) VIPR-ATR (0.3 mm x 0.3 mm x 1.0 mm effective voxel size with 3 slice averaging of 0.3 mm isotropic images in each dimension and 8 minute scan time). Signal-to-noise ratio (SNR) and contrast-to-noise ratio (CNR) efficiency measurements normalized to voxel volume were performed on all MRI examinations. Paired t-tests were used to compare differences in normalized SNR and CNR efficiency values between sequences. Two musculoskeletal radiologists independently reviewed all MRI examinations and ranked the sequences based upon the following subjective measures of image quality: 1) tissue contrast, 2) clarity of articular surface, 3) cartilage lesion conspicuity, and 4) overall assessment of articular cartilage.
**Results:** VIPR-ATR and HR VIPR-ATR produced high quality multi-planar images of the knee joint with bright synovial fluid following a single acquisition (Figure 1). VIPR-ATR and HR VIPR-ATR had similar ($p=0.08$-$0.26$) normalized cartilage SNR efficiency as FSE-Cube and IDEAL-SPGR and significantly higher ($p<0.05$) normalized cartilage SNR efficiency than IDEAL-GRASS. VIPR-ATR and HR VIPR-ATR had significantly higher ($p<0.05$) normalized synovial fluid SNR efficiency than FSE-Cube, IDEAL-GRASS, and IDEAL-SPGR. VIPR-ATR and HR VIPR-ATR had significantly higher ($p<0.05$) normalized CNR efficiency between cartilage and synovial fluid than FSE-Cube, IDEAL-GRASS, and IDEAL-SPGR, but significantly lower ($p<0.05$) normalized CNR efficiency between cartilage and bone marrow than FSE-Cube and IDEAL-SPGR. On subjective analysis, HR VIPR-ATR followed by VIPR-ATR had the highest ranks for tissue contrast, clarity of articular surface, cartilage lesion conspicuity, and overall assessment of articular cartilage (Figure 2).

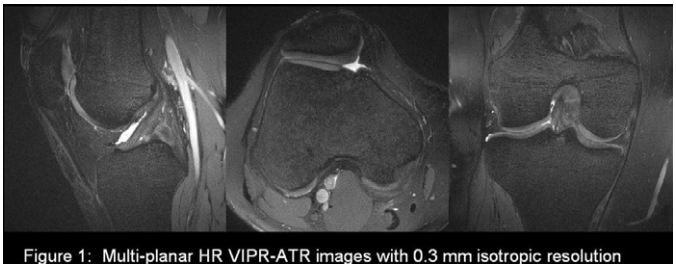

Figure 1: Multi-planar HR VIPR-ATR images with 0.3 mm isotropic resolution

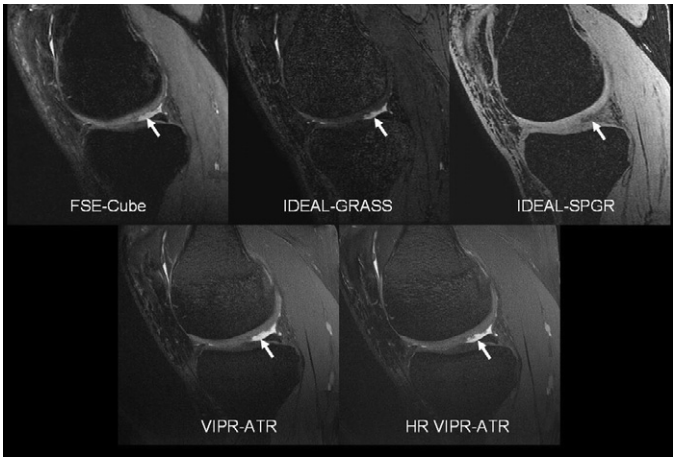


Figure 2: Appearance of a superficial partial-thickness cartilage lesion (arrows) on multiple high resolution cartilage imaging sequences

**Conclusions:** VIPR-ATR produces high quality multi-planar images of the knee joint with 0.4 mm isotropic resolution in 5 minutes and 0.3 mm isotropic resolution in 8 minutes. In contrast, the DESS sequence currently used in the Osteoarthritis Initiative to evaluate articular cartilage has a voxel size of 0.4 mm $\times$ 0.5 mm $\times$ 0.7 mm and a scan time of more than 10 minutes. VIPR-ATR images have high cartilage SNR efficiency and high contrast between cartilage and adjacent joint structures which makes them well suited for detecting cartilage lesions and for measuring cartilage volume. Since SSFP tissue contrast is also useful for evaluating menisci, ligaments, and osseous structures, VIPR-ATR may be used in osteoarthritis research studies to provide rapid "whole-organ" joint assessment and cartilage volume analysis.